Features of the appearance of secondary flows outside of a permeable cylinder rotating in a limited space

Mochalin E.V.

Donbass State Technical University, Alchevsk, Ukraine

Abstract

The flow of liquid outside of the revolved permeable cylinder with the channel of liquid through his side is considered. The analysis of flow features is made on the base of numerical solution of Reynolds averaged Navier - Stocks equations closed with SST k −ω turbulence model. It is rotined that the the turbulization of boundary layer on the surface of rotating cylinder and layer's thickness rising up to values close to the annular domain's height precedes the macro-vortex appearance. At that the centrifugal instability conditioned by secondary flows developing along the full height of annular domain, not within the thin laminar boundary layer.

Keywords: liquid; permeable cylinder; turbulence; vortex

1. Characteristics of the problem and objectives of the research

In technical applications, there is a flow outside a rotating permeable cylinder with a fluid flow through its side surface. An example is a rotary filter for the mechanical purification of liquids, in which the separation of suspended particles is carried out by a rotating perforated cylinder [1]. The study of such a flow is also of interest in order to improve power plants with rotating cylindrical bodies.

Monograph [2] systematizes known data on hydrodynamics and heat transfer outside an impermeable rotating cylinder during laminar and turbulent fluid motions. It is also indicated there that the flow through the surface of the cylinder (in terms of liquid suction) can introduce significant changes in the nature of the flow and the boundaries of the existence of various modes of motion. However, there are no well-established results known to a wide range of specialists in this case.

The task is complicated by the fact that the flow swirled by a rotating cylinder, limited by external walls, is prone to centrifugal buckling with the formation of spatial secondary flows. In this case, there is a nonuniform distribution of hydrodynamic characteristics near the surface of the cylinder in the axial direction. The flow between impermeable coaxial rotating cylinders and its particular case with a stationary outer cylinder are well studied [3,4]. In this case, the primary laminar circular Couette flow at sufficiently low angular velocities is replaced by macrovortex motion in the form of toroidal Taylor vortices. With a further increase in the angular velocity, each other is replaced by a number of laminar and turbulent macrovortex regimes. The influence of fluid suction through the surface of a rotating cylinder on the boundaries of the origin and nature of the macrovortex flow requires further study.

The flow closest to the type under consideration, for which the effect of liquid suction has been studied, is the flow in the boundary layer on a concave surface. A common circumstance is that near the surface of a rotating cylinder, there is an active (destabilizing) effect of centrifugal forces, just as in the case of a flow around a stationary concave surface [2]. In [77], the results of various authors on determining the critical Gertler number corresponding to the loss of stability of a laminar flow in a boundary layer on a concave surface are

*Corresponding author
email: y_mochalin@mail.ru
doi: https://doi.org/10.23877/MS.TS.39.005
Published online: 15 June 2017

© Mochalin E.V.

compared and compared with the available experimental data. At the same time, there is a significant scatter in the data of various authors and the following ratios are recommended:

$$\text{Gö}_{cr} = 22.97 \quad \left(\delta^{**}/R\right) \le 0.02,$$
$$\text{Gö}_{cr} = 22.76\left(\frac{\delta^{**}}{R}\right)^{0.0484} \quad \left(0.02 < \delta^{**}/R < 0.1\right) \quad (1)$$

where δ^{**} – impulse loss thickness, R – surface curvature radius, $\text{Gö} = \frac{V_e\delta^{**}}{\nu}\sqrt{\frac{\delta^{**}}{R}}$ – Gertler number, V_e – boundary layer velocity.

The results of the study of the stabilizing effect of liquid suction are summarized in [5] in the form of dependence

$$\frac{\text{Gö}_{cr}}{\text{Gö}_{cr\,0}} = 1 + 0.0277\left(\text{Re}_o^{**}\right)^{1.515},$$
$$\text{Re}_o^{**} = \frac{V_o\delta^{**}}{\nu} \quad (2)$$

where V_o – suction speed, ν – kinematic viscosity of the fluid, a Gö_{cr0} is defined by expressions (1).

The centrifugal instability, the boundaries of which are determined by equalities (1), (2), manifests itself in the form of Gertler vortices, elongated along the streamlined surface and concentrated inside the boundary layer.

The main feature of the boundary layer on the surface of a rotating permeable cylinder is the circumferential periodicity, which does not allow automatic use of dependences (1), (2).

Thus, the purpose of this work is to reliably determine the boundary of occurrence and the nature of secondary flows outside a rotating permeable cylinder (RPC) with liquid suction, as well as to assess the possibility of using known results for this.

2. Results and discussion

In [6], an analytical solution was obtained that determines the following profile of the circumferential velocity in an axisymmetric laminar motion outside the RPC when fluid is supplied through a stationary external permeable cylinder:

$$v_\varphi = \frac{\tilde{r}^{2-\text{Re}_r} - \left(1+\tilde{h}\right)^{2-\text{Re}_r}}{\tilde{r}\left(1-\left(1+\tilde{h}\right)^{2-\text{Re}_r}\right)} \quad (3)$$

where $v_\varphi = V_\varphi/W$ – dimensionless circumferential speed, $\tilde{r} = r/R$ – dimensionless radial coordinate, $\tilde{h} = h/R$ – dimensionless height of the annular region, R – RPC outer radius, $W = \Omega R$ – circumferential speed of the cylinder surface, Ω – its angular velocity, and the radial Reynolds number

$$\text{Re}_r = V_o R/\nu \quad (4)$$

determined by suction speed V_o.

As shown in [6], for $\text{Re}_r > 50$ instead of (3) you can use a simpler expression

$$v_\varphi = \tilde{r}^{1-\text{Re}_r} \quad (5)$$

In this case, the circumferential motion of the fluid is concentrated in the boundary layer on the rotating surface, and the outer fixed wall does not affect the velocity distribution.

For a dimensionless momentum loss thickness, from (5) we have

$$\tilde{\delta}^{**} = \int_1^\infty v_\varphi\left(1-v_\varphi\right)d\tilde{r} = \frac{\text{Re}_r - 1}{\left(2\,\text{Re}_r - 3\right)\left(\text{Re}_r - 2\right)} \quad (6)$$

The physical similarity of the considered type of flows is determined [7] by the characteristics of the forced motion of the fluid in each of the independent directions and the uneven distribution of inertia forces. The characteristics of the forced movement in the radial and circumferential directions are the radial (4) and rotational Reynolds numbers. The latter is defined as follows:

$$\text{Re}_\varphi = WR/\nu$$

There is no forced axial flow in the case under consideration.

The uneven distribution of inertial forces in the presence of a circumferential flow in the entire

annular gap height h (as is the case in the case of impermeable cylinders) characterizes the Taylor number

$$\mathrm{Ta} = \frac{\Omega R h}{\nu}\sqrt{\frac{h}{R}} = \mathrm{Re}_\varphi \tilde{h}\sqrt{\tilde{h}},$$

where $\tilde{h} = h/R$ – dimensionless height of the annular region.

In the presence of a boundary layer along peripheral speed, the Hertler number is used instead Ta, which in this case is defined as follows:

$$\mathrm{Gö} = \frac{\Omega R \delta^{**}}{\nu}\sqrt{\frac{\delta^{**}}{R}} = \mathrm{Re}_\varphi \tilde{\delta}^{**}\sqrt{\tilde{\delta}^{**}} \qquad (7)$$

However, due to (6) the number Gö expressed through Re_φ and Re_r. Instead of the latter, we will further use the dimensionless suction velocity (or the suction parameter)

$$v_o = V_o / W \qquad (8)$$

given the ratio

$$\mathrm{Re}_r = \mathrm{Re}_\varphi v_o \qquad (9)$$

In [8], from the point of view of the linear theory of hydrodynamic stability, neutral curves were constructed that determine the boundary of the loss of stability by the primary laminar flow outside the RPC with a circumferential velocity profile (3) (Figure 1). In this case, the stability with respect to small axisymmetric perturbations.

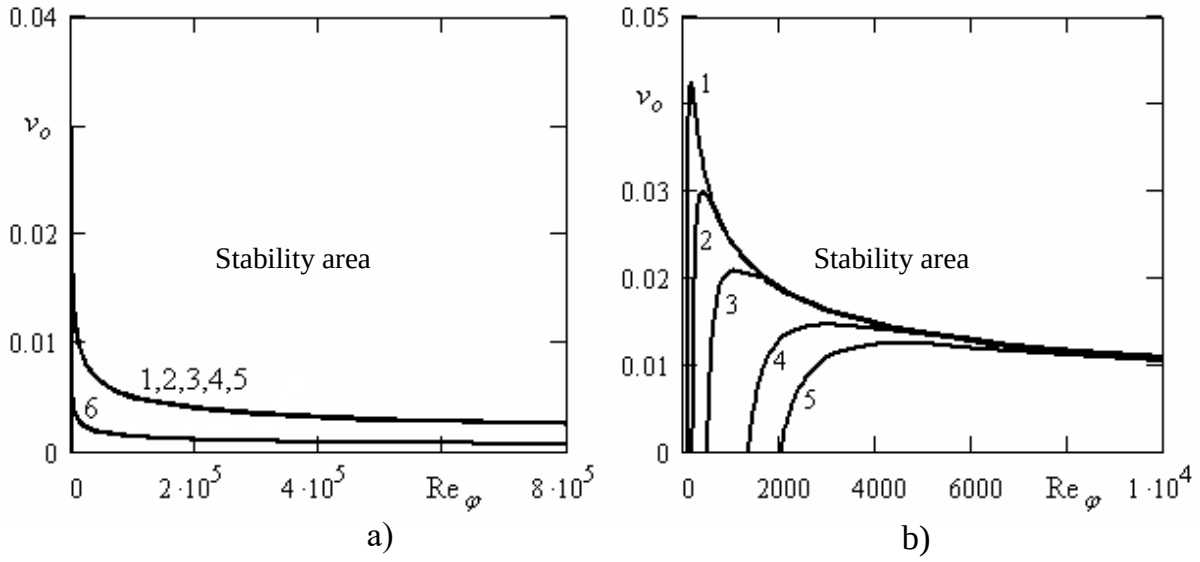

Figure 1. Neutral flow stability curves in the annular gap outside the RPC with liquid suction in the ranges $\mathrm{Re}_\varphi \le 8\cdot10^5$ (a) and $\mathrm{Re}_\varphi \le 1\cdot10^4$ (b): 1 – $\tilde{h} = 0.8048$; 2 – $\tilde{h} = 0.4024$; 3 – $\tilde{h} = 0.2012$; 4 – $\tilde{h} = 0.1006$; 5 – $\tilde{h} = 0.0768$; 7 – boundary layer on a concave surface with suction (formula (11))

As can be seen from the graphs, at ($\mathrm{Re}_\varphi > 10^4$) the neutral curve becomes universal, independent of the height of the annular region (h). In this range, it is well approximated by the expression

$$(v_o)_{cr} = 0.26\,\mathrm{Re}_\varphi^{-0.35} + 3.3\cdot10^{-4} \qquad (10)$$

If, with conditions (1), (2), which determine the boundary of the manifestation of centrifugal instability in the boundary layer on a concave surface with suction, use (rather conventionally) expression (6) for the momentum loss thickness, as well as equalities, (7), (9), then we come to the equation

$$\mathrm{Re}_\varphi\left(\frac{\mathrm{Re}_\varphi v_o - 1}{(2\,\mathrm{Re}_\varphi v_o - 3)(\mathrm{Re}_\varphi v_o - 2)}\right)^{1.5} = 22.97 + 0.636\left(\frac{\mathrm{Re}_\varphi v_o(\mathrm{Re}_\varphi v_o - 1)}{(2\,\mathrm{Re}_\varphi v_o - 3)(\mathrm{Re}_\varphi v_o - 2)}\right)^{1.515} \qquad (11)$$

The solution of this equation defines curve 7 in Figure 1.

The comparison shows that an attempt to use the results known for the boundary layer on a concave surface with suction when estimating the boundaries of centrifugal buckling outside the RPC leads to underestimated values of the critical suction velocity by more than 100% compared to a more consistent approximate solution.

As can be seen, at $\mathrm{Re}_\varphi > 10^4$ the critical suction velocity does not depend on the height of the annular region. In this case $\mathrm{Re}_r > 50$ and the thickness of the boundary layer in unperturbed motion is less than the height h. Linear analysis gives the most dangerous perturbations for the wavelength (causing at a given Re_φ loss of stability at the highest suction speeds v_o) values close to twice the height of the boundary layer ($2\pi/k \approx 2\tilde{\delta}$). In this case, the perturbations themselves are concentrated within the boundaries of the boundary layer. Thus, small axisymmetric perturbations develop in the manner of Gertler vortices. Verification and refinement of this result can be performed on the basis of detailed numerical simulation, which takes into account the nonlinearity of the initial equations and the possibility of turbulence development.

The paper [9] substantiates the approach to discretization of the Reynolds-averaged Navier-Stokes equations presented as the equations of momentum component transfer in a rotating cylindrical coordinate system ––

$$\frac{\partial(\rho V_{i)}}{\partial t} + \nabla\cdot\left(\rho V_i \mathbf{U}\right) = -\nabla p\cdot\mathbf{i}_i + \\ + \nabla\cdot\left(\mu_e \nabla V_i\right) + \nabla\cdot\left(\mu_e\left(\nabla V_j\cdot\mathbf{i}_i\right)\mathbf{i}_j\right) - \\ - \nabla\left(\frac{2}{3}\rho k\right)\cdot\mathbf{i}_i + S_i, \quad (i = 1,2,3) \qquad (12)$$

where $\mathbf{i}_i$ – unit vectors of axes of a cylindrical coordinate system, k – specific kinetic energy of turbulent fluctuations, μ_e – is the effective viscosity of the fluid, and the source terms S_i, due to the curvilinearity and mobility of the coordinate system are defined as follows:

$$S_1 = S_r = -\frac{1}{r^2}\frac{\partial\left(\mu_e V_\varphi\right)}{\partial\varphi} - \frac{2\mu_e}{r^2}\frac{\partial V_\varphi}{\partial\varphi} - \\ - \frac{2\mu_e V_r}{r^2} + \frac{\rho U_\varphi V_\varphi}{r} + \rho\Omega V_\varphi \quad ,$$

$$S_2 = S_\varphi = \frac{2}{r^2}\frac{\partial\left(\mu_e V_r\right)}{\partial\varphi} + \frac{\mu_e}{r}\frac{\partial V_\varphi}{\partial r} + \frac{\mu_e}{r^2}\frac{\partial V_r}{\partial\varphi} - \\ - \frac{\partial}{\partial r}\left(\frac{\mu_e V_\varphi}{r}\right) - \frac{2\mu_e V_\varphi}{r^2} - \frac{\rho U_\varphi V_r}{r} - \rho\Omega V_r \quad ,$$

$$S_3 = S_z = 0\,.$$

erification and testing demonstrate the reliability and good computational properties of the numerical solution obtained by the finite volume method.

It was shown in [10] that the use of the SST k – ω turbulence model (the Menter model) provides a unified computational approach to modeling the type of flow under study in a wide range of fluid motion regimes: from stable laminar to laminar and turbulent macrovortex motions. This provides an adequate calculation of the average characteristics of the fluid flow, including the possibility of predicting the local degeneration of turbulence under conditions of fluid suction through the surface of the RPC. Transfer Equations for Turbulence Characteristics (k, ω) have a structure similar to equations (12), and for their discretization a similar approach based on the finite volume technology is used. The full formulation of the Menter model is given, in particular, in [11].

The described approach to detailed numerical modeling is highly general and makes it possible to refine the above results on the stability of the flow outside the HCV, obtained in a linear approximation. To do this, we will consider the calculation scheme shown in Figure 2 and corresponding to the axisymmetric problem of the flow of an incompressible fluid between a stationary outer and rotating inner permeable cylinders. The liquid is supplied evenly through the perforated surface of the outer cylinder, and the liquid is discharged through the surface of the rotating cylinder (RPC).

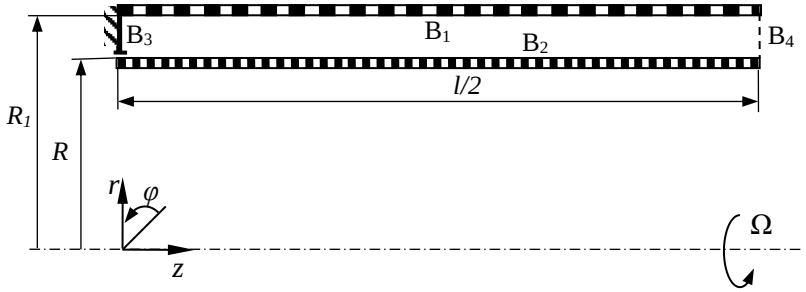

Figure 2. Calculation scheme of the fluid flow in the annular region between the stationary external and rotating internal uniformly permeable surfaces

The boundary conditions used are as follows:

$$\left.\begin{aligned}
&B_1:\ V_\varphi = V_z = 0,\ V_r = v_o \Omega R \frac{R}{R_1} = \frac{v_o W}{1+\tilde{h}},\ \frac{\partial k}{\partial n} = 0,\ \omega = 10\frac{6\mu}{\rho\beta_{i,1}\Delta y^2},\\
&B_2:\ V_z = 0,\ V_\varphi = W,\ V_r = v_o W,\ \frac{\partial k}{\partial n} = 0,\ \omega = 10\frac{6\mu}{\rho\beta_{i,1}\Delta y^2},\\
&B_3:\ V_r = V_\varphi = V_z = 0,\ \frac{\partial k}{\partial n} = 0,\ \omega = 10\frac{6\mu}{\rho\beta_{i,1}\Delta y^2},\\
&B_4:\ \frac{\partial V_r}{\partial z} = \frac{\partial V_\varphi}{\partial z} = \frac{\partial k}{\partial z} = \frac{\partial \omega}{\partial z} = 0,\ V_z = 0,
\end{aligned}\right\}$$

where Δy – near-wall grid spacing, $\beta_{i,1} = 0.075$ – Menter's turbulence model coefficient.

A structured rectangular computational grid is used for the calculation. The wall step is chosen equal to $\Delta y = 5\cdot 10^{-6} R$, which allows to have at least 10 grid nodes within the laminar sublayer for all investigated regimes. The model used makes it possible to observe the appearance and development of secondary flows, as well as the distribution of averaged turbulence characteristics.

It can be seen from Figure 3 that secondary flows in the form of macrovortices stably manifest themselves not within the limits of a thin laminar boundary layer, as follows from the linear analysis, but over the entire height of the annular region. This trend persists with an increase in the height of the annular region, at least for $\tilde{h} \le 0.2$.

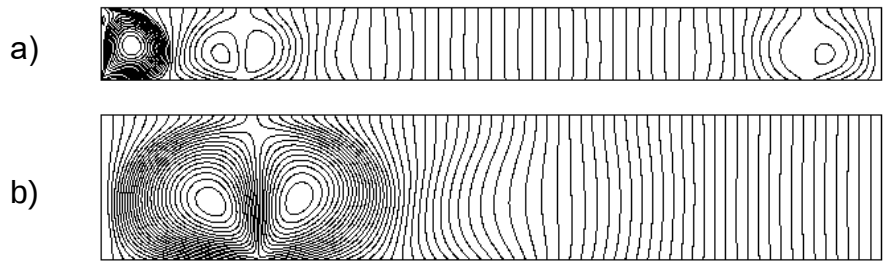

Figure 3. Streamlines of relative fluid motion ($\mathrm{Re}_\varphi = 2\cdot 10^5, v_o = 0.005$) at $\tilde{h} = 0.1$ (a) and $\tilde{h} = 0.2$ (b)

Nevertheless, the boundary of the appearance of macrovortices is quite well estimated by dependence (10), obtained by the methods of the linear theory of hydrodynamic stability (Figure 4).

Numerical analysis also shows that with decreasing liquid suction rate (v_o) from obviously large values to critical ones, turbulence develops in a thin laminar boundary layer before the appearance of macrovortices. The thickness of the turbulent

layer grows to values approaching the height of the annular region. And only after that, over the entire height of the annular region, as shown in Figure 3, secondary flows begin to appear in the form of quasi-Taylor macrovortices.

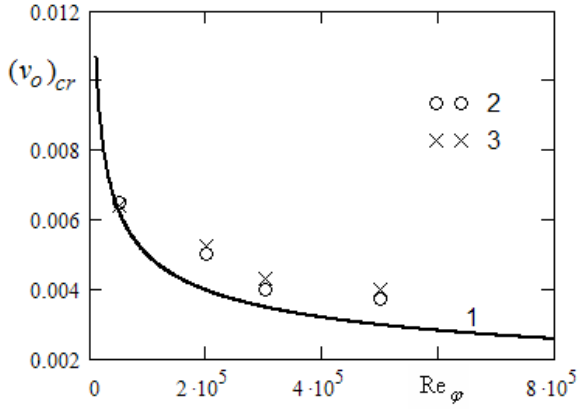

Figure 4. The boundary of the appearance of macrovortices in the annular region outside the RPC with liquid suction; 1 - dependence (10); 2 - numerical calculation $\tilde{h} = 0.1$; 3 – numerical calculation $\tilde{h} = 0.2$

This conclusion is illustrated by the graphs in Figure 5,6, where the distributions (profiles) of the dimensionless circumferential speed are presented (v_o) and relative turbulent viscosity ($\tilde{\nu}_t = \tilde{\nu}_t/\nu$) along the height of the annular area. For comparison, Figure 5 also shows the laminar velocity profile obtained analytically (formula (5)).

Figure s 7 - 9 illustrate the dependence of the circumferential velocity and turbulent viscosity profiles on the dimensionless height of the annular region $\tilde{h}$. The influence of the outer wall begins to manifest itself at a sufficiently large thickness of the boundary layer. For definiteness, we can say that significant differences in the profiles v_φ and especially) $\tilde{\nu}_t$ appear after the thickness of the boundary layer approaches half the height of the annular region for the smallest of the considered values $\tilde{h}$. However, as can be seen from Figure 4, this fact does not significantly affect the value $(v_o)_{cr}$, which determines the boundary of the occurrence of macrovortices. At the same time, for large $\tilde{h}$ turbulence level for values v_o, approaching $(v_o)_{cr}$, above.

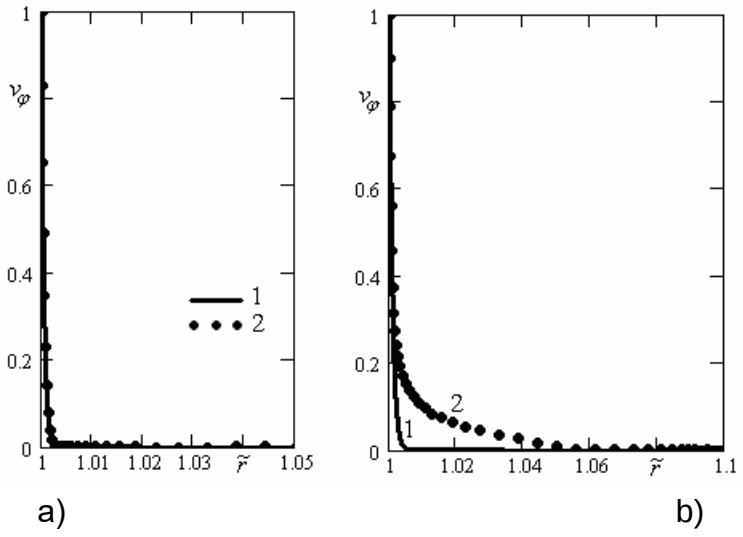

Figure 5. Profiles of dimensionless circumferential velocity outside a rotating permeable cylinder at $\mathrm{Re}_\varphi = 2\cdot10^5$, $v_o = 0.01$ (a) and $v_o = 0.0055$ (b): 1 – analytical solution (3.26), laminar model; 2 – numerical solution (Menter's turbulence model)

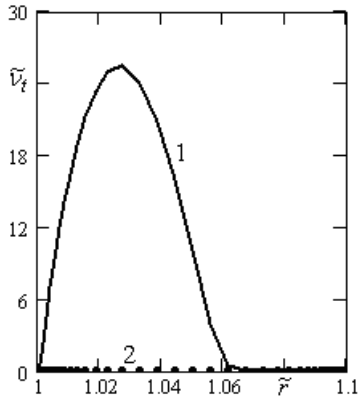

Figure 6. Relative turbulent viscosity profiles outside a rotating permeable cylinder at $\mathrm{Re}_{\varphi} = 2 \cdot 10^5$: 1 – $v_o = 0.0055$; 2 – $v_o = 0.01$

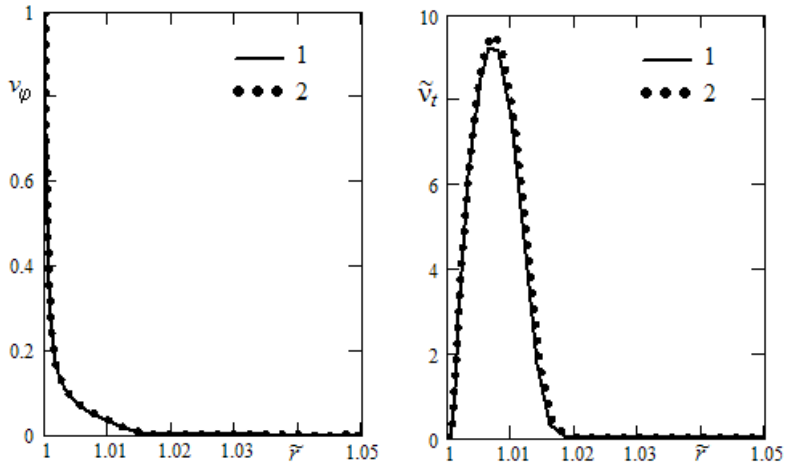

a) b)

Figure 7. Profiles of dimensionless circumferential velocity (a) and relative turbulent viscosity (b) at $\mathrm{Re}_{\varphi} = 2 \cdot 10^5, v_o = 0.0085$: 1 – $\tilde{h} = 0.1$; 2 – $\tilde{h} - 0.2$

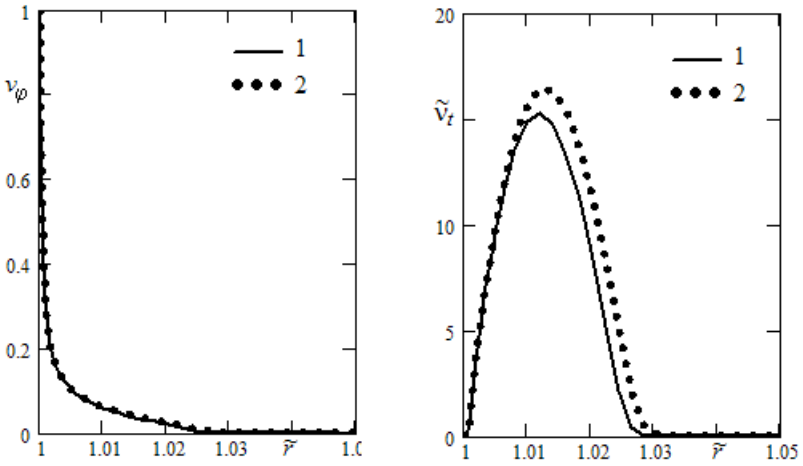

a) b)

Figure 8. Profiles of dimensionless circumferential velocity (a) and relative turbulent viscosity (b) at $\mathrm{Re}_{\varphi} = 2 \cdot 10^5, v_o = 0.0075$: 1 – $\tilde{h} = 0.1$; 2 – $\tilde{h} - 0.2$

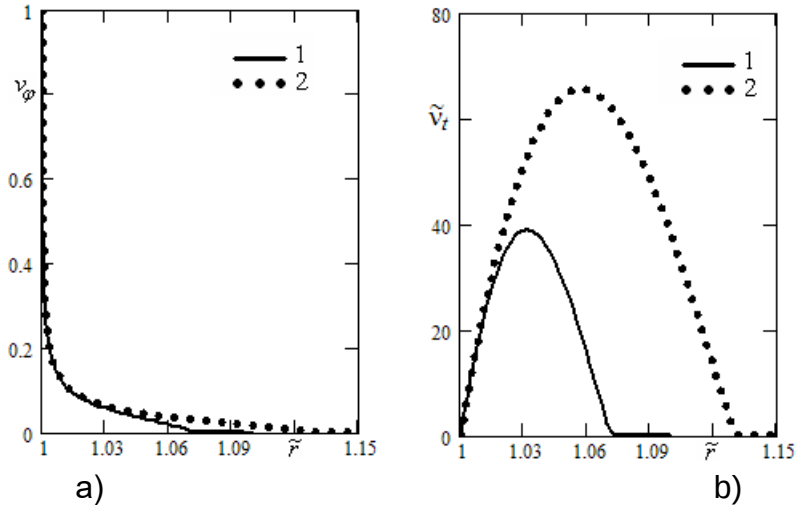

Figure 9. Profiles of dimensionless circumferential velocity (a) and relative turbulent viscosity (b) at $\mathrm{Re}_\varphi = 2\cdot 10^5, v_o = 0.006$: 1 – $\tilde{h} = 0.1$; 2 – $\tilde{h} - 0.2$

3. Conclusions

The performed research determined the boundary of centrifugal buckling of fluid flow outside a rotating permeable cylinder with fluid suction through its surface. The method of small perturbations is used to obtain a graphical representation and an analytical expression of the neutral stability curve, which determines the smallest (critical) values of the dimensionless suction velocity, corresponding to the appearance of secondary flows in the form of macrovortices. Computational analysis based on a detailed numerical solution of the Reynolds equations, closed on the basis of the SST k – ω turbulence model with a detailed resolution of the near-wall region, demonstrated the closeness of the critical values $(v_o)_{cr}$ to the results of linear analysis with a slight improvement in the direction of increasing these values in the region of large numbers Re_φ ($\mathrm{Re}_\varphi > 10^5$). In this case, the emergence of macrovortices is preceded by turbulence of the boundary layer on the surface of the rotating cylinder and an increase in its thickness to values close to the height of the annular region. With an increase in this height, the critical values of the suction velocity do not change significantly. Altitude effect $\tilde{h}$ on the profiles of the average circumferential velocity and turbulent viscosity appears only when the suction speed approaches v_o to critical values $(v_o)_{cr}$.

The results obtained can be used in the improvement of rotary filters for the mechanical purification of liquids, heat exchangers, rotary wind turbines, and some apparatuses for chemical and food technologies.

References

[1] Kovalenko V.P. Lubricating and hydraulic oils for the coal industry: A Handbook / V.P. Kovalenko, Z.L. Finkelstein. - M.: Nedra, 1991. - 294 p.

[2] Khalatov A.A. Heat transfer and hydrodynamics in the fields of centrifugal mass forces: in 4 tons / A.A. Khalatov, A.A. Avramenko, I.V. Shevchuk. - Kyiv: Institute of Tech. Thermophysics of the National Academy of Sciences of Ukraine, 1996. – V.2: Rotating systems. – 289 p..

[3] Taylor G.I. Stability of a viscous liquid contained between two rotating cylinders / G.I.Taylor // Phil.Trans.Roy. Soc.London. A.– 1923.– V.223.– P. 289 – 343.

[4] Coles D. Transition in circular Couette flow / D.Coles // J.Fluid Mech.– 1965–V.21.– P.385 – 425.

[5] Thermogasdynamics of complex flows near curved surfaces / [A.A.Khalatov, I.V.Shevchuk, A.A.Avramenko et al.]. - Kyiv: In-t tekhn. Thermal Physics of the National Academy of Sciences of Ukraine, 1999.– 300 p.

[6] Mochalin E.V. Fluid motion in the vicinity of a rotating permeable cylinder / E.V. Mochalin // Bulletin of the Khidnoukrainian National University. – 2003.– No. 12(68), Part 2.– P. 197 – 202..

[7] Khalatov A.A. Heat transfer and hydrodynamics in the fields of centrifugal mass forces: in 4 tons / A.A. Khalatov, A.A. Avramenko, I.V. Shevchuk. - Kyiv: Institute of Tech. Thermophysics of the National Academy of Sciences of Ukraine, 1996.– Vol. 1: Curvilinear flows. – 290 p.

[8] Mochalin E.V. Hydrodynamic stability in the working cavity of a rotary filter / E.V. Mochalin // Industrial hydraulics and pneumatics. - 2005. - No. 4 (10). - P. 50 – 54.

[9] Mochalin E.V. Numerical modeling of viscous fluid flows in the working cavity of a rotary filter / E.V. Mochalin // Sat. scientific Proceedings of DonSTU.– Alchevsk: DonSTU, 2007.– Issue. 23.– P. 169 – 183.

[10] Mochalin E.V. Selection of a turbulence model for the analysis of the flow outside a rotating permeable cylinder / E.V. Mochalin // Eastern European Journal of Advanced Technologies. - 2007. - No. 2/6 (26).

[11] Numerical modeling of vortex heat transfer intensification in tube bundles: / Yu.A. Bystrov, S.A. Isaev, N.A. Kudryavtsev, A.I.

© Мочалин Е.В.